

# Absolute coronary flow and microvascular resistance before and after transcatheter aortic valve implantation

Emanuele Gallinoro<sup>1,2</sup>, MD, PhD; Pasquale Paolisso<sup>1,2</sup>, MD, PhD; Dario Tino Bertolone<sup>1</sup>, MD; Giuseppe Esposito<sup>1,3</sup>, MD, PhD; Marta Belmonte<sup>1,3</sup>, MD; Attilio Leone<sup>1,3</sup>, MD; Michele Mattia Viscusi<sup>1,3</sup>, MD; Monika Shumkova<sup>1</sup>, MD; Cristina De Colle<sup>1</sup>, MD; Ivan Degrieck<sup>1</sup>, MD; Filip Casselman<sup>1</sup>, MD; Martin Penicka<sup>1</sup>, MD; Carlos Collet<sup>1</sup>, MD, PhD; Jeroen Sonck<sup>1</sup>, MD, PhD; Eric Wyffels<sup>1</sup>, MD; Jozef Bartunek<sup>1</sup>, MD, PhD; Bernard De Bruyne<sup>1,4</sup>, MD, PhD; Marc Vanderheyden<sup>1</sup>, MD; Emanuele Barbato<sup>1,5\*</sup>, MD, PhD

*E. Gallinoro and P. Paolisso contributed equally to this work.*

*\*Corresponding author: Department of Clinical and Molecular Medicine, Sapienza University of Rome, Piazzale Aldo Moro, 5, 00185, Rome, Italy. E-mail: emanuele.barbato@uniroma1.it*

*This paper also includes supplementary data published online at: <https://eurointervention.pronline.com/doi/10.4244/EIJ-D-24-00075>*

## ABSTRACT

**BACKGROUND:** Severe aortic stenosis (AS) is associated with left ventricular (LV) remodelling, likely causing alterations in coronary blood flow and microvascular resistance.

**AIMS:** We aimed to evaluate changes in absolute coronary flow and microvascular resistance in patients with AS undergoing transcatheter aortic valve implantation (TAVI).

**METHODS:** Consecutive patients with AS undergoing TAVI with non-obstructive coronary artery disease in the left anterior descending artery (LAD) were included. Absolute coronary flow (Q) and microvascular resistance ( $R_{\mu}$ ) were measured in the LAD using continuous intracoronary thermodilution at rest and during hyperaemia before and after TAVI, and at 6-month follow-up. Total myocardial mass and LAD-specific mass were quantified by echocardiography and cardiac computed tomography. Regional myocardial perfusion ( $Q_{N}$ ) was calculated by dividing absolute flow by the subtended myocardial mass.

**RESULTS:** In 51 patients, Q and R were measured at rest and during hyperaemia before and after TAVI; in 20 (39%) patients, measurements were also obtained 6 months after TAVI. No changes occurred in resting and hyperaemic flow and resistance before and after TAVI nor after 6 months. However, at 6-month follow-up, a notable reverse LV remodelling resulted in a significant increase in hyperaemic perfusion ( $Q_{N,hyper}$ : 0.86 [interquartile range [IQR] 0.691-1.06] vs 1.20 [IQR 0.99-1.32] mL/min/g;  $p=0.008$ ; pre-TAVI and follow-up, respectively) but not in resting perfusion ( $Q_{N,rest}$ : 0.34 [IQR 0.30-0.48] vs 0.47 [IQR 0.36-0.67] mL/min/g;  $p=0.06$ ).

**CONCLUSIONS:** Immediately after TAVI, no changes occurred in absolute coronary flow or coronary flow reserve. Over time, the remodelling of the left ventricle is associated with increased hyperaemic perfusion.

**KEYWORDS:** angina; ANOCA; aortic stenosis; CFR; coronary artery disease; flow reserve; microvascular dysfunction

Severe aortic stenosis (AS) is characterised by a progressive increase in afterload and wall stress, and secondary concentric remodelling<sup>1,2</sup>. These changes might ultimately provoke angina despite the absence of obstructive coronary artery disease.

When comparing absolute flow and resistance in patients with and without AS, we observed that with the progression of left ventricle (LV) hypertrophy (LVH), myocardial perfusion was maintained at rest but not during hyperaemia<sup>3</sup>.

By alleviating the resistance to flow, aortic valve implantation is supposed to improve myocardial perfusion and microcirculatory function. Due to the lack of accurate measures of volumetric flow and absolute microvascular resistance, the extent and time course of these changes have not been well defined<sup>4,5</sup>. The recent development of continuous intracoronary thermodilution to assess absolute coronary flow and resistance in an operator-independent manner<sup>6-8</sup> enables clinicians to better characterise the interplay between LV mass, flow and resistance in patients with AS.

The aim of the present study (unlike our previous one comparing flow and resistance in patients with and without severe AS<sup>3</sup>) is to explore the physiological changes in the microcirculatory function by using continuous intracoronary thermodilution to assess both resting and hyperaemic absolute coronary flow and microvascular resistance before transcatheter aortic valve implantation (TAVI), immediately after TAVI, and at 6-month follow-up.

Editorial, see page e1196

## Methods

### DESIGN AND STUDY POPULATION

In this observational, single-centre, prospective study, consecutive patients undergoing TAVI for symptomatic severe AS from June 2021 to January 2023 at the Cardiovascular Center Aalst (Aalst, Belgium) were considered eligible. Inclusion criteria were as follows: (1) presence of normal-flow, high-gradient severe AS; and (2) absence of significant epicardial stenosis in the left anterior descending artery (LAD; defined as diameter stenosis [DS] >50% by visual estimation). Exclusion criteria were the following: (1) previous myocardial infarction (MI); (2) previous coronary artery bypass graft (CABG) in the LAD territory; (3) valve-in-valve procedure; (4) left ventricular ejection fraction (LVEF) <50%; (5) low-flow, low-gradient AS; and (6) left bundle branch block or right ventricular pacing.

All patients underwent cardiac computed tomography (CCT), echocardiography, and left and right catheterisation as part of TAVI procedural planning (data concerning the left and right catheterisation are listed in **Supplementary Table 1**)<sup>9</sup>. Physiological assessments of flow and resistance were performed before and immediately after TAVI in all patients. Details about

### Impact on daily practice

Coronary microvascular dysfunction (CMD) is common among patients with severe aortic stenosis and has been shown to be related to the extent of extra-valvular cardiac damage. In the present study, we demonstrated that absolute resting and hyperaemic flow, as well as coronary flow reserve, remained unchanged before transcatheter aortic valve implantation (TAVI), after TAVI and at 6-month follow-up, likely reflecting irreversible structural damage of the microcirculation. Further investigations are needed to assess the prognostic impact of CMD in these patients and the potential role of microcirculatory function as a marker of early adverse cardiac remodelling requiring anticipated future interventions.

size and types of implanted valves are presented in **Supplementary Table 2**. Clinical follow-up was performed approximately at 6 months after TAVI with echocardiography and, in a subgroup of patients, also with coronary angiography and invasive physiological assessment with intracoronary continuous thermodilution. A detailed description of the echocardiographic protocol is provided in **Supplementary Appendix 1**. The protocol was approved by the institutional review board of the Onze-Lieve-Vrouw Clinic in Aalst, Belgium (registration number: 2021/033). The present study was conducted according to the Declaration of Helsinki; all patients were informed about their participation in the study and provided informed consent for the anonymous publication of scientific data. Patients were not involved in the research process.

### CORONARY ANGIOGRAPHY AND INVASIVE PHYSIOLOGICAL ASSESSMENT

Coronary catheterisation was performed through either radial or femoral access. A 6 Fr guiding catheter was used to cannulate the LAD. A guidewire equipped with a pressure/temperature sensor (PressureWire X [Abbott]) was connected to a dedicated software for tracings analysis (CoroFlow Cardiovascular System [Coroventis]) and, after zeroing, was advanced through the guiding catheter. The pressures recorded by the pressure/temperature wire and by the fluid-filled guide catheter were equalised close to the tip of the guiding catheter. Next, the wire was advanced into the distal part of the coronary artery. Thereafter, the distal coronary pressure to aortic pressure ratio (Pd/Pa) and resting full-cycle ratio (RFR) were recorded.

### CONTINUOUS INTRACORONARY THERMODILUTION

Absolute coronary blood flow and microvascular resistance were measured with continuous intracoronary thermodilution

### Abbreviations

<b>AS</b>	aortic stenosis	<b>LAD</b>	left anterior descending artery	<b>NHPR</b>	non-hyperaemic pressure ratio
<b>CABG</b>	coronary artery bypass graft	<b>LV</b>	left ventricle	<b>Q</b>	absolute coronary flow
<b>CCT</b>	cardiac computed tomography	<b>LVEF</b>	left ventricular ejection fraction	<b>R<sub>p</sub></b>	absolute microvascular resistance
<b>CFR</b>	coronary flow reserve	<b>MRR</b>	microvascular resistance reserve	<b>TAVI</b>	transcatheter aortic valve implantation

of saline through a dedicated monorail infusion microcatheter with 4 distal side holes (RayFlow [Hexacath]). The method has been already described elsewhere, and details are reported in **Supplementary Appendix 1**<sup>6,10-12</sup>.

Absolute coronary flow ( $Q$  in mL/min) and resistance ( $R_p$  in Wood units [WU]) as derived from continuous thermodilution were calculated by the previously validated equations both at rest ( $Q_{rest}$  and  $R_{p,rest}$ , respectively) and during hyperaemia ( $Q_{hyper}$  and  $R_{p,hyper}$ )<sup>10,13</sup>.

Coronary flow reserve (CFR) was calculated as the ratio between  $Q_{hyper}$  and  $Q_{rest}$ . Microvascular resistance reserve (MRR) was calculated as the ratio of CFR to fractional flow reserve (FFR) and corrected for the changes in systemic pressure as previously described<sup>14</sup>.

### CARDIAC COMPUTED TOMOGRAPHY, MYOCARDIAL MASS AND PERFUSION QUANTIFICATION

The myocardial mass quantification has been described in detail previously and is provided in **Supplementary Appendix 1**<sup>3</sup>. In brief, vessel-specific myocardial mass was quantified by the CCT images using Voronoi's algorithm with dedicated software (Synapse 3D [Fujifilm Healthcare Solutions])<sup>15</sup>. The values of the total LV myocardial mass, the vessel-specific myocardial mass, and the percentage of LAD mass for the total LV mass were exported. Myocardial perfusion at rest ( $Q_{N,rest}$ ) and during hyperaemia ( $Q_{N,hyper}$ ) were calculated by dividing absolute flow by the specific myocardial mass subtended by the LAD (calculated as the % of LAD mass obtained by CCT angiography on the total LV mass obtained by echocardiography). Myocardial perfusion at rest ( $Q_{N,rest}$ ) and during hyperaemia ( $Q_{N,hyper}$ ) were calculated by dividing absolute flow for the specific myocardial mass subtended by the LAD.

### STATISTICAL ANALYSIS AND SAMPLE SIZE CALCULATION

The distribution of continuous variables was assessed visually by histograms or the Shapiro-Wilk test as appropriate. Continuous variables with normal distribution are expressed as mean±standard deviation and non-normally distributed

variables as median (interquartile range). Categorical variables are expressed as count and percentages. Normal ranges are presented as the 5<sup>th</sup> and 95<sup>th</sup> percentiles. The Student's t-test and chi-square test were used to compare differences between continuous and categorical variables, respectively. Pearson's correlation coefficient and linear regression models were fitted to evaluate the association between continuous variables. Details about the sample size calculation are reported in **Supplementary Appendix 1**; based on an expected mean difference in CFR before and after TAVI of approximately 15-20% to achieve a power of 80% and a significance level of 5%, the minimum required sample size ranged between 19 and 34 patients.

All analyses were performed with R statistical software (R Foundation for Statistical Computing).  $P < 0.05$  was considered statistically significant.

## Results

### STUDY POPULATION

Between June 2021 and January 2023, we screened 117 patients referred for a TAVI procedure for inclusion in our study. Among them, 66 patients were excluded, and 51 patients were eventually included in the study (12 of whom were already included in our previous pilot study<sup>3</sup>). Invasive absolute flow measurements were performed in the following patients:

- The overall cohort (N=51) underwent absolute flow measurements at rest and during hyperaemia before and immediately after TAVI;
- A subgroup of 20 patients also had these measurements performed at 6-month follow-up.

The study flowchart is presented in **Figure 1**. In the overall population, the mean age was  $83.7 \pm 5.0$  years, and 16 were male (31.4%). The most prevalent clinical presentation was dyspnoea, in New York Heart Association Class II-III (92.2%); 9.8% of patients had angina, and 11.8% had syncope. Baseline characteristics of the overall population are summarised in **Table 1**; those of the subset of patients who underwent invasive

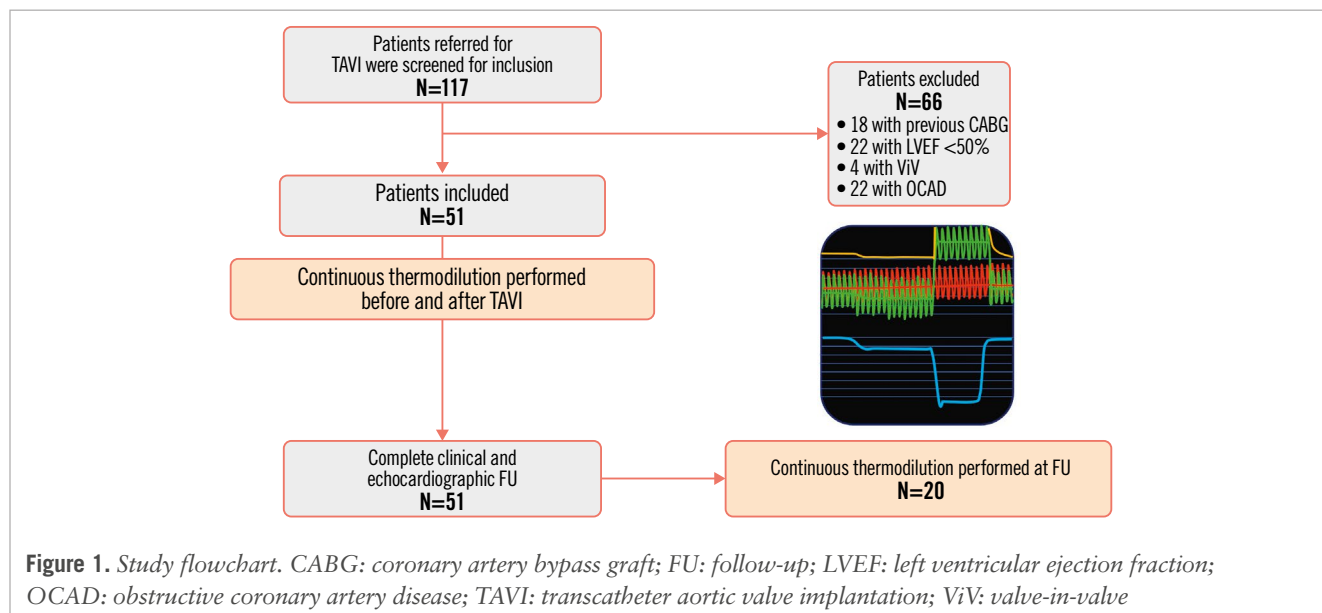


**Table 1. Baseline characteristics.**

Characteristic	N=51
Male sex	16 (31.4)
Age, years	83.7±5.0
BMI, kg/m <sup>2</sup>	26.0±5.3
Smoking habitus	9 (17.6)
Hypertension	43 (84.3)
Diabetes	16 (31.4)
Dyslipidaemia	42 (82.4)
Afib	4 (7.8)
History of Afib	17 (33.3)
Creatinine, mg/dL	1.07±0.74
GFR, mL/min/1.73 m <sup>2</sup>	62.71±19.38
CKD	16 (31.4)
History of CAD	10 (19.6)
Previous PCI	8 (15.7)
Previous MI	1 (2.0)
Pacemaker	3 (5.9)
Angina	5 (9.8)
Dyspnoea	49 (96.1)
Syncope	6 (11.8)
Previous HF hospitalisation	6 (11.8)
Diuretics	27 (52.9)
Antialdosteronics	10 (19.6)
ACEi/ARBs	25 (49.0)
Statins	38 (74.5)
Beta blockers	23 (45.1)
Calcium channel blockers	16 (31.4)
Insulin	3 (5.9)
OAD	14 (27.5)
Anticoagulation	14 (27.5)
Aspirin	17 (33.3)
P2Y <sub>12</sub> inhibitors	11 (21.6)

Data are expressed as number (percentage) or mean±standard deviation. ACEi: angiotensin-converting enzyme inhibitors; Afib: atrial fibrillation; ARBs: angiotensin II receptor blockers; BMI: body mass index; CAD: coronary artery disease; CKD: chronic kidney disease; GFR: glomerular filtration rate; HF: heart failure; MI: myocardial infarction; OAD: oral antidiabetics; PCI: percutaneous coronary intervention

physiological assessment at 6-month follow-up are shown in **Supplementary Table 3**.

#### ECHOCARDIOGRAPHIC DATA AND CARDIAC REMODELLING

All 51 patients completed clinical and echocardiographic follow-ups. The mean follow-up time was 6.1±1.3 months. Echocardiographic data are reported in **Supplementary Table 4**.

The mean transaortic pressure gradient was 51.5±10.2 mmHg, with a mean peak aortic jet velocity of 4.43±0.40 cm/s and a mean aortic valve area of 0.62±0.41 cm<sup>2</sup>. The mean LV myocardial mass was 201.9±37.9 g, with 72.5% of patients presenting with concentric LVH. Echocardiographic data at discharge are shown in **Supplementary Table 5**.

At follow-up, there was a significant reduction in left ventricular mass of approximately 13% (from 201.9±37.9 g to 175.1±46.6 g; p<0.001) with a decrease of the septal thickness (from 14.0±1.7 mm to 11.8±1.9 mm; p<0.001). Consequently, the percentage of patients with LVH decreased from 72.5% to 51.0% (p=0.041).

#### PRE- AND IMMEDIATELY POST-TAVI FLOW ASSESSMENT

Absolute flow and resistance measurements pre- and post-TAVI are listed in **Table 2**.

There were no acute changes in either resting Pd/Pa or RFR after TAVI (Pd/Pa: 0.91±0.03 vs 0.91±0.04; p=0.768; RFR: 0.87±0.05 vs 0.85±0.06; p=0.081, pre- and post-TAVI respectively). Similarly, the FFR values before and after TAVI were similar (0.84±0.06 vs 0.83±0.06, respectively; p=0.339).

Resting flow values were similar before and immediately after TAVI (68 [56-88] mL/min vs 69 [55-92] mL/min; p=0.776) as well as the hyperaemic flow values (159 [129-201] mL/min vs 172 [132-216] mL/min; p=0.449) (**Supplementary Figure 1**). As a result, both CFR and MRR remained unchanged (CFR: 2.38±0.79 vs 2.47±0.97; p=0.875; and MRR: 2.72±0.97 vs 2.96±1.17; p=0.361, pre- and immediately post-TAVI, respectively) (**Supplementary Figure 1**).

#### LONG-TERM CHANGES AFTER TAVI

In 20 patients, physiological assessment was repeated at 6-month follow-up after TAVI. Overall, resting Pd/Pa and RFR did not significantly change between baseline and follow-up (Pd/Pa: 0.91±0.03 vs 0.92±0.04; p=0.788; RFR: 0.88±0.03 vs 0.87±0.06; p=0.553, pre-TAVI and follow-up, respectively). Similarly, no significant changes were noted in FFR values at follow-up compared to pre-TAVI values (0.83±0.05 vs 0.84±0.07; p=0.795, respectively).

Values of absolute flow and resistance measurements at baseline and at follow-up are reported in **Table 3**.

Resting absolute flow and microvascular resistance were similar at baseline and follow-up ( $Q_{rest}$ : 72 [63-84] vs 83 [59-108] mL/min; p=0.658;  $R_{h,rest}$ : 1,083 [767-1,268] vs 916 [725-1,481] WU; p=0.925; pre-TAVI and follow-up, respectively) (**Figure 2**). Similarly, no changes occurred in terms of hyperaemic flow and resistance ( $Q_{hyper}$ : 181 [158-201] vs 194 [166-223] mL/min; p=0.492;  $R_{h,hyper}$ : 413 [353-482] vs 389 [341-524] WU; p=0.869; pre-TAVI and follow-up, respectively). Consequently, both CFR and MRR remained unchanged at follow-up (CFR: 2.45±0.76 vs 2.71±0.97; p=0.388; MRR: 2.78±0.88 vs 2.73±0.97; p=0.854, pre-TAVI and follow-up, respectively). Accordingly, there was a weak correlation between the relative increase in CFR and the relative change in myocardial mass between baseline and follow-up (**Supplementary Figure 2**).

However, in terms of myocardial perfusion, a significant increase was observed in hyperaemic perfusion between pre-TAVI and follow-up ( $Q_{N,hyper}$ : 0.86 [0.69-1.06] vs 1.20 [0.99-1.32] mL/min/g; p=0.008; pre-TAVI and follow-up, respectively) (**Figure 2**). Resting perfusion showed a numerically but not statistically significant increase at follow-up ( $Q_{N,rest}$ : 0.34 [0.30-0.48] vs 0.47 [0.36-0.64] mL/min/g; p=0.061). When comparing the relative changes in myocardial mass and myocardial perfusion at rest and during hyperaemia (**Figure 3**), the regression model showed that

**Table 2. Absolute flow and resistance measurements collected pre- and post-TAVI.**

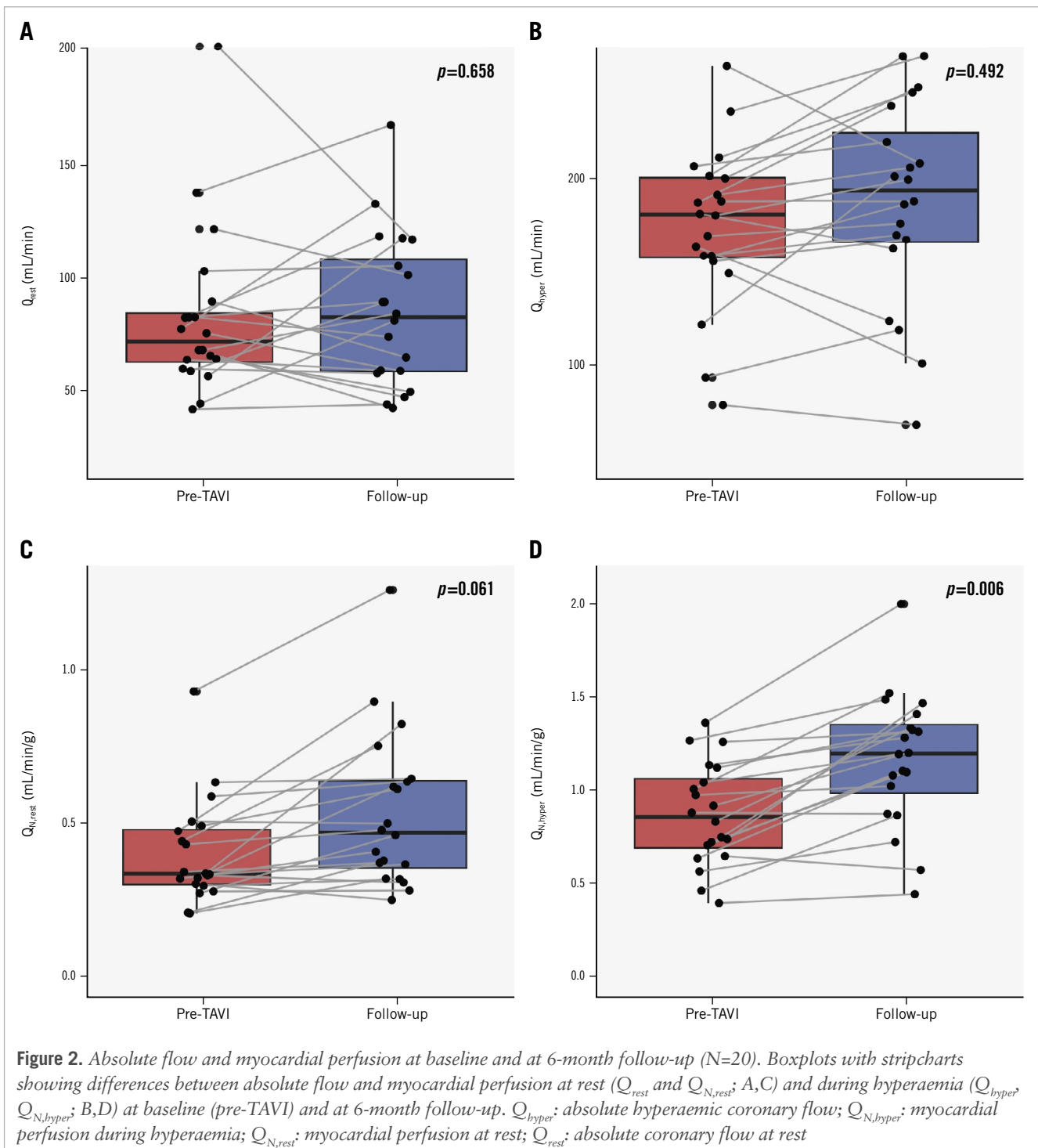
	Pre-TAVI (N=51)	Post-TAVI (N=51)	p-value
Pd <sub>rest</sub>	76±19	77±14	0.261
Pa <sub>rest</sub>	83±19	85±13	0.184
Pd/Pa	0.91±0.03	0.91±0.04	0.768
RFR	0.87±0.05	0.85±0.06	0.081
Q <sub>rest</sub> † mL/min	68 [56-88]	69 [55-92]	0.776
R <sub>μ,rest</sub> † WU	1,145 [796-1,277]	1,147 [822-1,299]	0.944
Pd <sub>hyper</sub>	72±15	72±15	0.973
Pa <sub>hyper</sub>	86±16	87±16	0.611
FFR	0.84±0.06	0.83±0.06	0.339
Q <sub>hyper</sub> † mL/min	159 [129-201]	172 [132-216]	0.449
R <sub>μ,hyper</sub> † WU	438 [370-532]	422 [332-520]	0.458
CFR	2.38±0.79	2.47±0.97	0.875
MRR	2.72±0.97	2.96±1.17	0.361
Q <sub>N,rest</sub> † mL/min/g	0.34 [0.27-0.50]	0.38 [0.29-0.45]	0.710
Q <sub>N,hyper</sub> † mL/min/g	0.75 [0.63-1.05]	0.85 [0.71-1.08]	0.349
R <sub>μ,N,rest</sub> † WU/g	5.53 [3.78-6.90]	5.44 [3.80-7.75]	0.880
R <sub>μ,N,hyper</sub> † WU/g	2.17 [1.83-2.87]	2.13 [1.60-3.04]	0.529
CPP, mmHg	42.3±14.1	37.6±18.1	0.152
LVEDP, mmHg	17.1±8.0	18.1±7.3	0.443

Data are presented as mean±standard deviation or median [interquartile range]. CFR: coronary flow reserve; CPP: coronary perfusion pressure; FFR: fractional flow reserve; LVEDP: left ventricular end-diastolic pressure; MRR: microvascular resistance reserve; Pa: aortic pressure; Pd: distal coronary pressure; Q<sub>hyper</sub>: absolute hyperaemic coronary flow; Q<sub>N,hyper</sub>: myocardial perfusion during hyperaemia; Q<sub>N,rest</sub>: myocardial perfusion at rest; Q<sub>rest</sub>: absolute coronary flow at rest; RFR: resting full-cycle ratio; R<sub>μ,N,hyper</sub>: microvascular hyperaemic resistance normalised for myocardial mass; R<sub>μ,N,rest</sub>: microvascular resistance at rest normalised for myocardial mass; R<sub>μ,hyper</sub>: absolute microvascular resistance during hyperaemia; R<sub>μ,rest</sub>: absolute microvascular resistance at rest; TAVI: transcatheter aortic valve implantation; WU: Wood units

**Table 3. Absolute flow and resistance measurements at baseline and at 6-month follow-up.**

	Pre-TAVI (N=20)	Follow-up (N=20)	p-value
Pd <sub>rest</sub>	79±26	78±14	0.791
Pa <sub>rest</sub>	87±26	84 ±12	0.755
Pd/Pa	0.91±0.03	0.92±0.04	0.788
RFR	0.88±0.03	0.87±0.06	0.553
Pd <sub>hyper</sub>	75±17	76±13	0.942
Pa <sub>hyper</sub>	89±19	90±15	0.859
FFR	0.84±0.07	0.83±0.05	0.795
Q <sub>rest</sub> † mL/min	72 [63-84]	83 [59-108]	0.658
Q <sub>hyper</sub> † mL/min	181 [158-201]	194 [166-223]	0.492
R <sub>μ,rest</sub> † WU	1,083 [767-1,268]	916 [725-1,481]	0.925
R <sub>μ,hyper</sub> † WU	413 [353-482]	389 [341-524]	0.869
CFR	2.45±0.76	2.71±0.97	0.338
MRR	2.78±0.88	2.73±0.97	0.854
LV mass, g	208±47	164±24	<0.001
LV mass indexed, g/m <sup>2</sup>	118±23	100±34	<0.001
Q <sub>N,rest</sub> † mL/min/g	0.34 [0.30-0.48]	0.47 [0.36-0.64]	0.061
Q <sub>N,hyper</sub> † mL/min/g	0.86 [0.69-1.06]	1.20 [0.99-1.32]	0.008
R <sub>μ,N,rest</sub> † WU/g	5.05 [3.97-6.84]	5.61 [4.47-9.03]	0.256
R <sub>μ,N,hyper</sub> † WU/g	2.09 [1.76-2.89]	2.31 [2.05-3.20]	0.304

Data are presented as mean±standard deviation or median [interquartile range]. CFR: coronary flow reserve; FFR: fractional flow reserve; LV: left ventricular; LVEDP: left ventricular end-diastolic pressure; MRR: microvascular resistance reserve; Pa: aortic pressure; Pd: distal coronary pressure; Q<sub>hyper</sub>: absolute hyperaemic coronary flow; Q<sub>N,hyper</sub>: myocardial perfusion during hyperaemia; Q<sub>N,rest</sub>: myocardial perfusion at rest; Q<sub>rest</sub>: absolute coronary flow at rest; RFR: resting full-cycle ratio; R<sub>μ,N,hyper</sub>: microvascular hyperaemic resistance normalised for myocardial mass; R<sub>μ,N,rest</sub>: microvascular resistance at rest normalised for myocardial mass; R<sub>μ,hyper</sub>: absolute microvascular resistance during hyperaemia; R<sub>μ,rest</sub>: absolute microvascular resistance at rest; TAVI: transcatheter aortic valve implantation; T<sub>hyper</sub>: mixed temperature during hyperaemia; T<sub>i,hyper</sub>: infusion temperature during hyperaemia; T<sub>i,rest</sub>: infusion temperature at rest; T<sub>rest</sub>: mixed temperature at rest; WU: Wood units

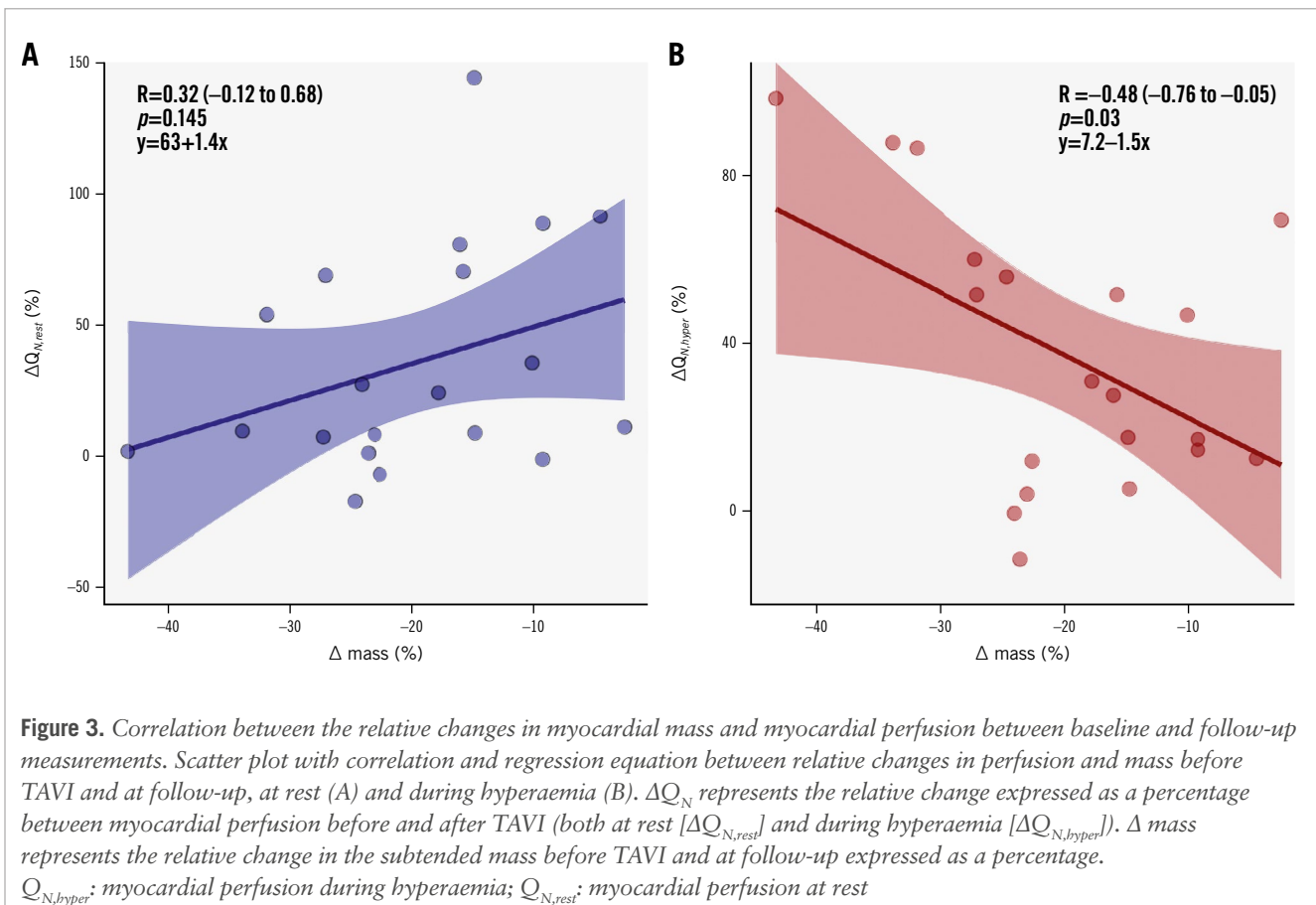


despite changes in myocardial mass, the resting perfusion did not change significantly ( $R=0.32$  [-0.12 to 0.68];  $p=0.145$ ). However, there was a significant inverse linear correlation between LV remodelling and the hyperaemic perfusion ( $R=-0.48$  [-0.76 to -0.05];  $p=0.03$ ), the latter increasing along with a decrease in LV myocardial mass.

## Discussion

In the present study, we collected the largest dataset concerning absolute coronary flow and microvascular resistance at

rest and during hyperaemia in patients with AS before and after TAVI, and at 6-month follow-up. The findings of our study can be summarised as follows (**Central illustration**): (1) no immediate changes occurred in terms of flow and flow reserve post-TAVI, and this remained consistent at 6-month follow-up; (2) TAVI induces a significant reverse remodelling of the LV with a significant reduction in the global myocardial mass; and (3) consequently, this reverse remodelling results in a significant improvement of hyperaemic perfusion at follow-up.



### ACUTE HAEMODYNAMIC CHANGES AFTER TAVI

In the haemodynamic model of aortic stenosis, the anatomical position of the valve precedes the coronary arteries resulting in increased afterload and reduced coronary perfusion pressure. It is theoretically expected that TAVI, by alleviating this obstruction, would acutely result in a significant increase in coronary perfusion pressure, thus enhancing coronary blood flow.

The evidence so far, however, remains controversial. One study utilising Doppler measurements supported this theoretical paradigm by showing an “instantaneous” effect of transcatheter aortic valve implantation on coronary flow velocities. This resulted in an increase in the hyperaemic average peak velocity and a decrease in hyperaemic microvascular resistance, while resting flow and resistance remained unchanged<sup>16</sup>. Furthermore, the observed changes were even more pronounced after excluding those patients with aortic regurgitation post-TAVI, resulting in a global increase of flow reserve. However, these findings were not confirmed by two small studies which showed that CFR was not affected by the immediate reduction in LV afterload after TAVI<sup>17,18</sup>.

In our study, utilising a direct and quantitative assessment of coronary flow in mL/min, we found no significant acute changes in terms of absolute flow or microvascular resistance neither at rest nor during hyperaemia after TAVI, leaving both CFR and MRR substantially unchanged. Stated another way, the immediate impact of TAVI on coronary haemodynamics appears to be negligible, suggesting that the exertional angina experienced, despite the absence of coronary artery stenosis,

cannot be fully attributed to a reduced coronary flow but rather to a mismatch between coronary blood flow and the increase in LV mass resulting from the concentric remodelling induced by the elevated afterload.

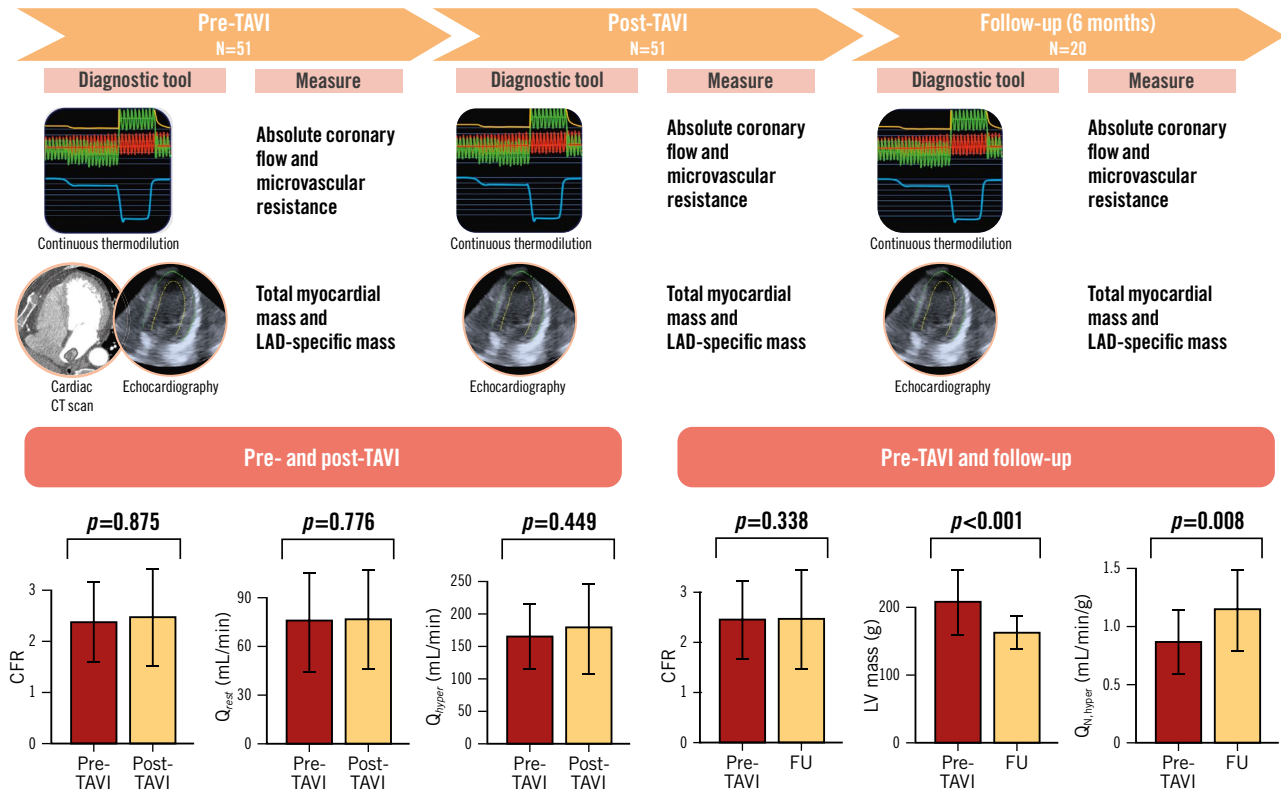
### LONG-TERM CHANGES AFTER TAVI

As previously shown, aortic valve stenosis, by increasing the afterload, triggers a compensatory mechanism of concentric remodelling of the LV which aims to reduce the heightened wall stress. Consequently, at rest, coronary autoregulation works to augment coronary flow in order to maintain an adequate perfusion. However, during hyperaemia, these autoregulatory mechanisms are unable to increase coronary flow to a level that would provide sufficient myocardial perfusion for the increased left ventricular mass<sup>3</sup>.

So far, the results of studies assessing long-term changes in coronary haemodynamics after TAVI have been inconclusive. While earlier studies suggested that hyperaemic coronary blood flow increases acutely immediately after TAVI and also tends to increase over time after the procedure<sup>19</sup>, others have shown that resting coronary flow decreases while hyperaemic flow remains constant<sup>20</sup>.

In our study, we did not observe at follow-up any significant changes either in resting or in hyperaemic absolute coronary flow, resulting in an unchanged CFR. Notably, myocardial perfusion at rest remained unchanged, whereas hyperaemic perfusion significantly increased, mainly driven by the reverse remodelling of the LV rather than an increase in absolute hyperaemic flow (**Figure 3**).

## Summary and main results of the study.



Emanuele Gallinoro *et al.* • *EuroIntervention* 2024;20:e1248-e1258 • DOI: 10.4244/EIJ-D-24-00075

CFR: coronary flow reserve; CT: computed tomography; FU: follow-up; LAD: left anterior descending artery; LV: left ventricular;  $Q_{hyper}$ : hyperaemic absolute coronary flow;  $Q_{N,hyper}$ : myocardial perfusion during hyperaemia;  $Q_{rest}$ : resting absolute coronary flow; TAVI: transcatheter aortic valve implantation

### PRACTICAL CONSIDERATIONS AND CLINICAL IMPLICATIONS

In the context of the pathophysiological changes observed in coronary microcirculation in patients with AS after TAVI, our study suggests that the reverse LV remodelling has a more significant impact than the acute LV unloading achieved by replacing the valve itself. The reverse remodelling plays a crucial role in improving hyperaemic myocardial perfusion and ensuring an adequate oxygen supply to the myocardium.

As mentioned previously, it was anticipated that patients undergoing TAVI would experience a decrease in baseline perfusion due to both acute changes in LV filling pressures and long-term regression of LV hypertrophy; however, among published studies, only one showed a decrease in resting parameters<sup>20</sup>. Despite the limitation of the small sample sizes, these studies, along with ours, do not demonstrate a substantial impact of TAVI on resting perfusion. These results highlight the remarkable ability of autoregulation to compensate for significant pathophysiological changes under resting conditions<sup>21</sup>, with the primary impact of TAVI only being observed at follow-up during hyperaemic conditions.

Second, the controversial and inconclusive results reported in previous studies may be attributed to the heterogeneity of the tools used to assess coronary microcirculation. In our study, we employed continuous intracoronary thermodilution, which is more operator independent and characterised by a lower intraobserver variability compared to intracoronary Doppler and bolus thermodilution<sup>22-24</sup>. This variation in assessment methods may explain the divergent outcomes observed in our study compared to others<sup>20</sup>.

Third, it has been shown that coronary microvascular dysfunction in patients with severe AS is associated with advanced extravalvular cardiac damage and that coronary abnormalities detected in an end-stage of the natural history of AS might be a sign of adverse remodelling and disease severity<sup>5,25</sup>. Yet, in the present study, despite the reverse remodelling observed at follow-up, absolute flow and resistance as well as CFR and MRR remained unchanged, likely reflecting irreversible structural damage of the coronary microcirculation.

Finally, the value reported for resting myocardial perfusion (median 0.34 mL/min/g) appears to be relatively low compared

to prior animal and human studies. This discrepancy might be related to (i) the selected study population of old patients with severe AS, LV hypertrophy, and likely a certain degree of myocardial fibrosis, which is hardly comparable with populations of previously published studies; and (ii) the method adopted for calculating the mass used to normalise the absolute flow. Specifically, we tried to solve an apparent divergence (likely due to LV concentric hypertrophy driven by AS) that was found between CT and echocardiography-derived myocardial mass (**Supplementary Figure 3**) by combining the two methods (**Supplementary Appendix 1**). On the other hand, it should be acknowledged that the main finding of our study regarding myocardial perfusion was the variation between baseline and 6-month follow-up; therefore, changing the method for relative mass derivation would not have challenged the robustness of this result, as the method remained the same for each timepoint of the study and for each patient.

### AORTIC STENOSIS, CORONARY FLOW AND FUNCTIONAL INDICES

Another important clinical implication of our study pertains to the ongoing debate concerning the use of resting and hyperaemic pressure indices to evaluate the functional severity of epicardial stenosis in patients with aortic stenosis. The findings from different studies have been contradictory, with some studies suggesting that the non-hyperaemic pressure ratio (NHPR) may be less affected by AS, while more recent studies have demonstrated that FFR is a more stable and reliable index in this specific subgroup of patients<sup>19,26-30</sup>.

As previously demonstrated, patients with AS often experience concentric remodelling which can lead to an increase in absolute resting flow compared to healthy control patients<sup>3</sup>. This increase in flow may affect the accuracy of resting pressure indices such as the NHPR. However, in our study, we did not observe any changes in NHPR or FFR after aortic valve implantation, which likely reflects the absence of significant changes in terms of absolute resting and hyperaemic flow.

What implications do these findings have for clinical practice? It is undeniably evident that the debate concerning the accuracy of FFR and NHPR in this subset of patients is far from settled, even considering our results. Notably, the recent ACTIVATION trial, which assessed the benefit of percutaneous coronary intervention (PCI) prior to transcatheter aortic valve implantation, demonstrated no benefit but instead an increased risk of bleeding for patients undergoing PCI prior to TAVI<sup>31</sup>. Therefore, it may be advisable to defer the physiological assessment and treatment of intermediate coronary stenosis until after the TAVI procedure, in order to avoid any potential bias related to the presence of AS.

### Limitations

Although our study was adequately powered based on an anticipated mean difference in CFR before and after TAVI of approximately 15-20%, the final sample size, particularly for the subgroup undergoing follow-up assessment, remained small. This limitation precluded us from conducting specific subanalyses, thus necessitating further validation of our findings through larger-scale studies. In addition,

approximately 60% of patients did not undergo a second coronary angiography at follow-up; in most cases, advanced age and patient frailty, along with the absence of symptoms, were among the primary reasons leading patients to decline a second coronary angiography, which, although recommended, was not mandatory for study enrolment.

Furthermore, the method we used to calculate myocardial perfusion, by normalising the absolute flow and myocardial mass subtended by the LAD, is based on the evidence of a strict correlation between flow and mass<sup>32-34</sup>, but still needs further validation from larger studies with positron emission tomography-derived resting myocardial flow, both in normal patients as well as in specific settings such as patients with AS and LVH.

Finally, we opted to exclude patients with reduced ejection fraction, including those with low-flow, low-gradient aortic stenosis, who often exhibit microvascular dysfunction<sup>35,36</sup>. This decision aimed to mitigate the confounding influence of reduced ejection fraction on coronary microcirculation<sup>37</sup>. Consequently, our findings are applicable solely to patients with normal-flow, high-gradient aortic stenosis.

### Conclusions

There were no significant differences observed in absolute resting and hyperaemic coronary blood flow before, immediately after, and – in a small subgroup of 20 patients – at 6 months after TAVI in patients with severe aortic valve stenosis. Similarly, perfusion at rest remained unchanged over time. However, hyperaemic perfusion increased with time in patients with reverse LV remodelling. These findings suggest that coronary autoregulation remained preserved/intact at the different timepoints and cannot solely explain the underlying cause of exercise-induced angina in AS. Nevertheless, the inverse relationship between perfusion and regression of LVH during hyperaemia suggests that a mismatch between perfusion and LV mass could contribute to this phenomenon. It implies that the hyperaemic perfusion may not be sufficient to meet the demands of the increased LV mass in AS patients, leading to the development of symptoms.

These observations highlight the complex interplay between coronary perfusion, LV remodelling and exercise-induced angina in patients undergoing TAVI. Further investigations are needed to better understand the mechanisms involved and identify strategies to optimise the timing of interventions to alleviate symptoms in this patient population.

### Authors' affiliations

1. Cardiovascular Center Aalst, OLV Clinic, Aalst, Belgium;
2. Division of University Cardiology, IRCCS Galeazzi - Sant' Ambrogio Hospital, Milan, Italy;
3. Department of Advanced Biomedical Sciences, University of Naples Federico II, Naples, Italy;
4. Department of Cardiology, Lausanne University Hospital, Lausanne, Switzerland;
5. Department of Clinical and Molecular Medicine, Sapienza University of Rome, Rome, Italy

### Conflict of interest statement

P. Paolisso, D.T. Bertolone, G. Esposito, M. Belmonte, A. Leone, and M.M. Viscusi are supported by a research grant from the CardioPaTh PhD programme. E. Barbato

declares speaker fees from Abbott, Boston Scientific, and GE HealthCare. C. Collet reports receiving research grants from Biosensors, GE HealthCare, Medis Medical Imaging, Pie Medical Imaging, CathWorks, Boston Scientific, Siemens, HeartFlow, and Abbott; and consultancy fees from HeartFlow, Opsens, Pie Medical Imaging, Abbott, and Philips. B. De Bruyne has institutional consulting relationships with Boston Scientific, Abbott, CathWorks, Siemens, GE HealthCare, and Coroventis Research; receives institutional research grants from Abbott, Coroventis Research, CathWorks, and Boston Scientific; and holds minor equities in Philips, Siemens, GE HealthCare, Edwards Lifesciences, HeartFlow, Opsens, and Celiad. The other authors have no conflicts of interest to declare.

## References

- Vahanian A, Beyersdorf F, Praz F, Milojevic M, Baldus S, Bauersachs J, Capodanno D, Conradi L, De Bonis M, De Paulis R, Delgado V, Freemantle N, Haugaa KH, Jeppsson A, Jüni P, Pierard L, Prendergast BD, Sádaba JR, Tribouilloy C, Wojakowski W. 2021 ESC/EACTS Guidelines for the management of valvular heart disease. *EuroIntervention*. 2022;17:e1126-96.
- McConkey HZR, Marber M, Chiribiri A, Pibarot P, Redwood SR, Prendergast BD. Coronary Microcirculation in Aortic Stenosis. *Circ Cardiovasc Interv*. 2019;12:e007547.
- Paolisso P, Gallinoro E, Vanderheyden M, Esposito G, Bertolone DT, Belmonte M, Mileva N, Bermpeis K, De Colle C, Fabricatore D, Candreva A, Munhoz D, Degrieck I, Casselman F, Penicka M, Collet C, Sonck J, Mangiacapra F, de Bruyne B, Barbato E. Absolute coronary flow and microvascular resistance reserve in patients with severe aortic stenosis. *Heart*. 2022;109:47-54.
- Kern MJ, Seto AH. Understanding the mechanism of improved CFR after TAVR/SAVR - the importance of basal flow. *EuroIntervention*. 2023;18:1129-30.
- Scarsini R, Gallinoro E, Ancona MB, Portolan L, Paolisso P, Springhetti P, Della Mora F, Mainardi A, Belmonte M, Moroni F, Ferri LA, Bellini B, Russo F, Vella C, Bertolone DT, Pesarini G, Benfari G, Vanderheyden M, Montorfano M, De Bruyne B, Barbato E, Ribichini F. Characterisation of coronary microvascular dysfunction in patients with severe aortic stenosis undergoing TAVI. *EuroIntervention*. 2024;20:e289-300.
- Candreva A, Gallinoro E, Fernandez Peregrina E, Sonck J, Keulards DCJ, Van't Veer M, Mizukami T, Pijls NHJ, Collet C, De Bruyne B. Automation of intracoronary continuous thermodilution for absolute coronary flow and microvascular resistance measurements. *Catheter Cardiovasc Interv*. 2022;100:199-206.
- Candreva A, Gallinoro E, van 't Veer M, Sonck J, Collet C, Di Gioia G, Kodeboina M, Mizukami T, Nagumo S, Keulards D, Fournier S, Pijls NHJ, De Bruyne B. Basics of Coronary Thermodilution. *JACC Cardiovasc Interv*. 2021;14:595-605.
- van 't Veer M, Adjedj J, Wijnbergen I, Tóth GG, Rutten MC, Barbato E, van Nunen LX, Pijls NH, De Bruyne B. Novel monorail infusion catheter for volumetric coronary blood flow measurement in humans: in vitro validation. *EuroIntervention*. 2016;12:701-7.
- Dweck MR, Loganath K, Bing R, Treibel TA, McCann GP, Newby DE, Leipzig J, Fracarro C, Paolisso P, Cosyns B, Habib G, Cavalcante J, Donal E, Lancellotti P, Clavel MA, Otto CM, Pibarot P. Multi-modality imaging in aortic stenosis: an EACVI clinical consensus document. *Eur Heart J Cardiovasc Imaging*. 2023;24:1430-43.
- Gallinoro E, Candreva A, Colaiori I, Kodeboina M, Fournier S, Nelis O, Di Gioia G, Sonck J, van 't Veer M, Pijls NHJ, Collet C, De Bruyne B. Thermodilution-derived volumetric resting coronary blood flow measurement in humans. *EuroIntervention*. 2021;17:e672-9.
- Gallinoro E, Candreva A, Fernandez-Peregrina E, Bailleul E, Meeus P, Sonck J, Bermpeis K, Bertolone DT, Esposito G, Paolisso P, Heggermont W, Adjedj J, Barbato E, Collet C, De Bruyne B. Saline-induced coronary hyperemia with continuous intracoronary thermodilution is mediated by intravascular hemolysis. *Atherosclerosis*. 2022;352:46-52.
- Belmonte M, Gallinoro E, Pijls NHJ, Bertolone DT, Keulards DCJ, Viscusi MM, Storozhenko T, Mizukami T, Mahendiran T, Seki R, Fournier S, de Vos A, Adjedj J, Barbato E, Sonck J, Damman P, Keeble T, Fawaz S, Gutiérrez-Barrios A, Paradies V, Bouisset F, Kern MJ, Fearon WF, Collet C, De Bruyne B. Measuring Absolute Coronary Flow and Microvascular Resistance by Thermodilution: JACC Review Topic of the Week. *J Am Coll Cardiol*. 2024;83:699-709.
- van't Veer M, Geven MC, Rutten MC, van der Horst A, Aarnoudse WH, Pijls NH, van de Vosse FN. Continuous infusion thermodilution for assessment of coronary flow: theoretical background and in vitro validation. *Med Eng Phys*. 2009;31:688-94.
- De Bruyne B, Pijls NHJ, Gallinoro E, Candreva A, Fournier S, Keulards DCJ, Sonck J, Van't Veer M, Barbato E, Bartunek J, Vanderheyden M, Wyffels E, De Vos A, El Farissi M, Tonino PAL, Muller O, Collet C, Fearon WF. Microvascular Resistance Reserve for Assessment of Coronary Microvascular Function: JACC Technology Corner. *J Am Coll Cardiol*. 2021;78:1541-9.
- Malkasian S, Hubbard L, Dertli B, Kwon J, Molloy S. Quantification of vessel-specific coronary perfusion territories using minimum-cost path assignment and computed tomography angiography: Validation in a swine model. *J Cardiovasc Comput Tomogr*. 2018;12:425-35.
- Wiegerinck EM, van de Hoef TP, Rolandi MC, Yong Z, van Kesteren F, Koch KT, Vis MM, de Mol BA, Piek JJ, Baan J Jr. Impact of Aortic Valve Stenosis on Coronary Hemodynamics and the Instantaneous Effect of Transcatheter Aortic Valve Implantation. *Circ Cardiovasc Interv*. 2015;8:e002443.
- Stoller M, Gloekler S, Zbinden R, Tueller D, Eberli F, Windecker S, Wenaweser P, Seiler C. Left ventricular afterload reduction by transcatheter aortic valve implantation in severe aortic stenosis and its prompt effects on comprehensive coronary haemodynamics. *EuroIntervention*. 2018;14:166-73.
- Camuglia AC, Syed J, Garg P, Kiaii B, Chu MW, Jones PM, Bainbridge D, Teffy PJ. Invasively assessed coronary flow dynamics improve following relief of aortic stenosis with transcatheter aortic valve implantation. *J Am Coll Cardiol*. 2014;63:1808-9.
- Vendrik J, Ahmad Y, Eftekhari A, Howard JP, Wijntjens GWM, Stegheuis VE, Cook C, Terkelsen CJ, Christiansen EH, Koch KT, Piek JJ, Sen S, Baan J Jr. Long-Term Effects of Transcatheter Aortic Valve Implantation on Coronary Hemodynamics in Patients With Concomitant Coronary Artery Disease and Severe Aortic Stenosis. *J Am Heart Assoc*. 2020;9:e015133.
- Sabbah M, Olsen NT, Holmvang L, Tilsted HH, Pedersen F, Joshi FR, Sørensen R, Jabbari R, Arslani K, Sondergaard L, Engstrøm T, Lønborg JT. Long-term changes in coronary physiology after aortic valve replacement. *EuroIntervention*. 2023;18:1156-64.
- Johnson NP, Gould KL, De Bruyne B. Autoregulation of Coronary Blood Supply in Response to Demand: JACC Review Topic of the Week. *J Am Coll Cardiol*. 2021;77:2335-45.
- Gallinoro E, Bertolone DT, Fernandez-Peregrina E, Paolisso P, Bermpeis K, Esposito G, Gomez-Lopez A, Candreva A, Mileva N, Belmonte M, Mizukami T, Fournier S, Vanderheyden M, Wyffels E, Bartunek J, Sonck J, Barbato E, Collet C, De Bruyne B. Reproducibility of bolus versus continuous thermodilution for assessment of coronary microvascular function in patients with ANOCA. *EuroIntervention*. 2023;19:e155-66.
- Gallinoro E, Bertolone DT, Mizukami T, Paolisso P, Bermpeis K, Munhoz D, Sakai K, Seki R, Ohashi H, Esposito G, Caglioni S, Mileva N, Leone A, Candreva A, Belmonte M, Storozhenko T, Viscusi MM, Vanderheyden M, Wyffels E, Bartunek J, Sonck J, Barbato E, Collet C, De Bruyne B. Continuous vs Bolus Thermodilution to Assess Microvascular Resistance Reserve. *JACC Cardiovasc Interv*. 2023;16:2767-77.
- Kodeboina M, Nagumo S, Munhoz D, Sonck J, Mileva N, Gallinoro E, Candreva A, Mizukami T, Van Durme F, Heyse A, Wyffels E, Vanderheyden M, Barbato E, Bartunek J, De Bruyne B, Collet C. Simplified Assessment of the Index of Microvascular Resistance. *J Interv Cardiol*. 2021;2021:9971874.
- Belmonte M, Paolisso P, Bertolone DT, Viscusi MM, Gallinoro E, de Oliveira EK, Shumkova M, Beles M, Esposito G, Addeo L, Botti G, Moya A, Leone A, Wyffels E, De Bruyne B, van Camp G, Bartunek J,

- Barbato E, Penicka M, Vanderheyden M. Combined Cardiac Damage Staging by Echocardiography and Cardiac Catheterization in Patients With Clinically Significant Aortic Stenosis. *Can J Cardiol*. 2024;40:643-54.
26. Ahmad Y, Götberg M, Cook C, Howard JP, Malik I, Mikhail G, Frame A, Petraco R, Rajkumar C, Demir O, Iglesias JF, Bhindi R, Koul S, Hadjiilouzou N, Gerber R, Ramrakha P, Ruparella N, Sutaria N, Kanaganayagam G, Ariff B, Fertleman M, Anderson J, Chukwumeka A, Francis D, Mayet J, Serruys P, Davies J, Sen S. Coronary Hemodynamics in Patients With Severe Aortic Stenosis and Coronary Artery Disease Undergoing Transcatheter Aortic Valve Replacement: Implications for Clinical Indices of Coronary Stenosis Severity. *JACC Cardiovasc Interv*. 2018;11:2019-31.
  27. Sabbah M, Joshi FR, Minkkinen M, Holmvang L, Tilsted HH, Pedersen F, Ahtarovski K, Sørensen R, Thue Olsen N, Søndergaard L, De Backer O, Engström T, Lønborg J. Long-Term Changes in Invasive Physiological Pressure Indices of Stenosis Severity Following Transcatheter Aortic Valve Implantation. *Circ Cardiovasc Interv*. 2022;15:e011331.
  28. Scarsini R, Lunardi M, Venturi G, Pighi M, Tavella D, Pesarini G, Ribichini F. Long-term variations of FFR and iFR after transcatheter aortic valve implantation. *Int J Cardiol*. 2020;317:37-41.
  29. Scarsini R, Pesarini G, Lunardi M, Piccoli A, Zanetti C, Cantone R, Bellamoli M, Ferrero V, Gottin L, Faggian G, Ribichini F. Observations from a real-time, iFR-FFR “hybrid approach” in patients with severe aortic stenosis and coronary artery disease undergoing TAVI. *Cardiovasc Revasc Med*. 2018;19:355-9.
  30. Scarsini R, Pesarini G, Zivelonghi C, Piccoli A, Ferrero V, Lunardi M, Gottin L, Zanetti C, Faggian G, Ribichini F. Physiologic evaluation of coronary lesions using instantaneous wave-free ratio (iFR) in patients with severe aortic stenosis undergoing transcatheter aortic valve implantation. *EuroIntervention*. 2018;13:1512-9.
  31. Patterson T, Clayton T, Dodd M, Khawaja Z, Morice MC, Wilson K, Kim WK, Meneveau N, Hambrecht R, Byrne J, Carrié D, Fraser D, Roberts DH, Doshi SN, Zaman A, Banning AP, Eltchaninoff H, Le Breton H, Smith D, Cox I, Frank D, Gershlick A, de Belder M, Thomas M, Hildick-Smith D, Prendergast B, Redwood S; ACTIVATION Trial Investigators. ACTIVATION (Percutaneous Coronary Intervention prior to transcatheter aortic valve implantation): A Randomized Clinical Trial. *JACC Cardiovasc Interv*. 2021;14:1965-74.
  32. Everaars H, de Waard GA, Schumacher SP, Zimmermann FM, Bom MJ, van de Ven PM, Raijmakers PG, Lammertsma AA, Götte MJ, van Rossum AC, Kurata A, Marques KMJ, Pijls NHJ, van Royen N, Knaapen P. Continuous thermodilution to assess absolute flow and microvascular resistance: validation in humans using [15O]H<sub>2</sub>O positron emission tomography. *Eur Heart J*. 2019;40:2350-9.
  33. Fournier S, Keulards DCJ, van 't Veer M, Colaiori I, Di Gioia G, Zimmermann FM, Mizukami T, Nagumo S, Kodeboina M, El Farissi M, Zelis JM, Sonck J, Collet C, Pijls NHJ, De Bruyne B. Normal values of thermodilution-derived absolute coronary blood flow and microvascular resistance in humans. *EuroIntervention*. 2021;17:e309-16.
  34. Keulards DCJ, Fournier S, van 't Veer M, Colaiori I, Zelis JM, El Farissi M, Zimmermann FM, Collet C, De Bruyne B, Pijls NHJ. Computed tomographic myocardial mass compared with invasive myocardial perfusion measurement. *Heart*. 2020;106:1489-94.
  35. Scarsini R, Portolan L, Della Mora F, Fabroni M, Andreaggi S, Mainardi A, Springhetti P, Dotto A, Del Sole PA, Fezzi S, Pazzi S, Tavella D, Mammone C, Lunardi M, Pesarini G, Benfari G, Ribichini FL. Coronary microvascular dysfunction in patients undergoing transcatheter aortic valve implantation. *Heart*. 2024;110:603-12.
  36. Scarsini R, Pighi M, Mainardi A, Portolan L, Springhetti P, Mammone C, Della Mora F, Fanti D, Tavella D, Gottin L, Bergamini C, Benfari G, Pesarini G, Ribichini FL. Proof of concept study on coronary microvascular function in low flow low gradient aortic stenosis. *Heart*. 2023;109:785-93.
  37. Paolisso P, Gallinoro E, Belmonte M, Bertolone DT, Bermpeis K, De Colle C, Shumkova M, Leone A, Caglioni S, Esposito G, Fabbicatore D, Moya A, Delrue L, Penicka M, De Bruyne B, Barbato E, Bartunek J, Vanderheyden M. Coronary Microvascular Dysfunction in Patients With Heart Failure: Characterization of Patterns in HFrEF Versus HFpEF. *Circ Heart Fail*. 2024;17:e010805.

## Supplementary data

**Supplementary Appendix 1.** Extended methods.

**Supplementary Table 1.** Results from the right heart catheterisation performed in the overall cohort (N=51).

**Supplementary Table 2.** Types and sizes of implanted valves.

**Supplementary Table 3.** Baseline characteristics of the patients who underwent invasive physiological assessment at follow-up compared to the overall cohort.

**Supplementary Table 4.** Echocardiographic data at baseline and at follow-up in the overall population.

**Supplementary Table 5.** Echocardiographic data at discharge.

**Supplementary Figure 1.** Absolute flow, myocardial perfusion, CFR and MRR pre- and post-TAVI in the overall population (N=51).

**Supplementary Figure 2.** Correlation between the relative changes in myocardial mass and myocardial perfusion between baseline and follow-up measurements.

**Supplementary Figure 3.** Divergence between CT and echocardiography-derived myocardial masses.

The supplementary data are published online at:

<https://eurointervention.pconline.com/>

doi/10.4244/EIJ-D-24-00075



## Supplementary data

### Supplementary Appendix 1. Extended methods.

#### *Sample Size Calculation*

Our study aims to assess whether TAVI induces a significant change in CFR in patients with severe AS. Therefore, in case of matched samples and using a continuous variable as main outcome the sample size can be calculated as following:

$$n = \left[ \frac{(Z_{1-\alpha/2} + Z_{1-\beta})}{ES} \right]^2$$

Where  $\alpha$  is the level of significance (set a 0.05),  $\beta$  is the power (0.80) and  $Z_{1-\alpha/2}$  and  $Z_{1-\beta}$  are the standard normal values given  $1-\alpha/2$  (as for a two-tailed test) and  $1-\beta$ .

The Effect Size (ES) is the expected effect of our treatment and is calculated as

$$ES = \frac{\mu_d}{\sigma_d}$$

where  $\mu_d$  is the mean difference expected under the alternative hypothesis,  $H_1$ , and  $\sigma_d$  is the standard deviation of the difference in the outcome (e.g., the difference based on measurements over time or the difference between matched pairs).

Therefore, based on the available data (1-4): assuming an increase of approximately 15 to 20% in CFR (difference of 0.34 to 0.46 units) and an estimated  $\sigma_d$  0.7 the minimum sample size would range between 19 and 34 patients.

#### *Echocardiography*

Comprehensive Transthoracic echocardiography (TTE) was performed as part of routine clinical practice using a high-quality ultrasound system (GE E95 or GE S70, GE Healthcare Horten, Norway) with a 3.5-MHz-phased array transducer (M5S). Echocardiographic examinations were performed following the recommendations of the American Society of Echocardiography and the European Association of Cardiovascular Imaging. All images were

stored for offline analysis by a cardiologist experienced in cardiac imaging, blinded to the invasive findings. Data were analyzed offline using dedicated software (EchoPAC PC SW-Only, version 202, GE Healthcare, Milwaukee, WI, USA). Left ventricular ejection fraction (LVEF) was calculated using Simpson's biplane method. LV mass was calculated with the corrected formula of the American Society of Echocardiography (ASE) and was indexed to BSA (1). Accordingly, LV hypertrophy has been assigned in the case of LV mass/BSA(g/m<sup>2</sup>) > 95 in women and > 115 in men.

Left ventricle reverse remodelling after TAVI was defined as the presence in echocardiographic assessment at follow-up of: i) a decrease  $\geq 20\%$  of LVMI and/or ii) a decrease  $\geq 20\%$  of LVEDV and/or iii) an improvement  $\geq 10\%$  of LVEF.

Peak aortic velocity was recorded using continuous-wave Doppler in several acoustic windows (apical 5-chamber). The highest aortic velocity was used to calculate aortic time-velocity integral, mean pressure gradient (MPG), and  $V_{\max}$ . AVA was calculated by the continuity equation. According to the results of peak velocity, MPG and AVA severity of aortic valve stenosis was assessed. LV diastolic function was evaluated by E, e' velocities, E/e', left atrial volume index (LAVi), and tricuspid regurgitation velocity. Determination of LV diastolic function was made using the algorithm proposed by the guidelines.

### ***Continuous Intracoronary thermodilution***

Absolute coronary blood flow and microvascular resistance were measured with continuous intracoronary thermodilution of saline through a dedicated monorail infusion 2.52 F microcatheter with 4 distal side holes (RayFlow®, Hexacath, Paris, France) The RayFlow® was connected to the 200-cc motorized syringe of an automated injection system (Medrad® Stellant, Medrad Inc, Warrendale, PA, USA) filled with saline at room temperature (typically between 20 and 23°C); then the microcatheter was advanced over the pressure/temperature

wire and its tip positioned into the first millimetres of the vessel. The temperature recorded was zeroed before starting saline infusion. Absolute resting ( $Q_{rest}$ ) and hyperaemic ( $Q_{hyp}$ ) flow measurements were obtained by using a saline infusion rate of 10 and 20 mL/min, respectively. The infusion pump was automatically programmed – as previously described - to (i) infuse saline at 10 mL/min for 2 minutes for the measurement of the temperature of blood mixed with infused saline (T); then (ii) to switch automatically to 20 mL/min for 1.5 minutes for the measurement of the temperature of blood mixed with infused saline (T) as well as – after a swift pullback of the temperature-sensor – for the measurement of hyperaemic saline infusion temperature ( $T_i$ ); and (iii) to switch back to 10 mL/min for 1 minute for the measurement of resting  $T_i$ . These techniques allowed for the calculation of resting and hyperaemic flow and resistance in one single procedure.

Absolute coronary flow (Q, mL/min) as derived from continuous thermodilution was calculated by the previously validated equation:

$$Q = 1.08 \cdot \frac{T_i}{T} \cdot Q_i \quad (1)$$

Where  $Q_i$  is the infusion rate of saline. Absolute resistance at rest ( $R_{\mu, rest}$ ) and during hyperaemia ( $R_{\mu, hyper}$ ) in Woods Units (WU) were calculated as the ratio between the distal coronary pressure during each infusion ( $P_d$ ) and  $Q_{rest}$  or  $Q_{hyper}$ , respectively. Coronary Flow Reserve (CFR), was calculated as the ratio between  $Q_{hyper}$  and  $Q_{rest}$ . MRR was calculated as previously described:

$$MRR = \frac{CFR}{FFR} \cdot \frac{P_{a, rest}}{P_{a, hyper}} \quad (2)$$

After aortic valve implantations, coronary angiography, invasive physiological assessment and continuous thermodilution measurements were repeated.

### **Cardiac computed tomography, myocardial mass and perfusion quantification**

CCT was performed with a dual-source CT scanner (Somatom Force 2 x 192-slice, Siemens, Germany) according to the protocol recommended by the Society of Cardiovascular Computed Tomography. Vessel-specific myocardial mass was quantified by the CCT images using the Voronoi's algorithm with a dedicated software (Synapse 3D, Fujifilm Healthcare Solutions, Holdings America Corporation). A voxel in the LV myocardium was linked to the nearest voxel on the adjacent coronary artery. Subsequently the algorithm automatically calculates the territory by aggregating all myocardial voxels associated to the voxels of the coronary artery that are distal to the target point. The values of the total LV myocardial mass, the vessel-specific myocardial mass and the percentage of LAD mass on the total LV mass were exported.

Myocardial perfusion at rest ( $Q_{N-rest}$ ) and during hyperaemia ( $Q_{N-hyp}$ ) were calculated by dividing absolute flow for the specific myocardial mass subtended by the LAD.

### ***TAVI Procedure***

The procedure was performed under awake sedation in all the patients.

Right femoral access for valve delivery and left femoral access for aortic root angiography were first obtained.

In patients undergoing balloon-expandable valve implantation left femoral vein was cannulated to place a stimulating catheter in the right ventricle whereas for self-expandable valve, pacing was performed over the wire.

The main femoral access was pre-closed with two suture-based vascular closure devices (ProGlide, Abbott, Abbott Park, Illinois).

The TAVI delivery sheath was inserted into the main access using a stiff wire. Then a Judkin Left 4 (JL4) guiding catheter was introduced in the TAVI delivery sheath to cannulate the left

coronary artery to perform the invasive physiological assessment. Afterward, using an Amplatz left (AL 1) catheter and a standard straight-tipped metallic wire the aortic valve was crossed, the catheter advanced into the LV and the straight-tipped wire was removed for an exchange length J-shaped wire. A pigtail catheter was placed in exchange for the catheter in the LV and directed towards the LV apex. At this time, simultaneous pressure assessment in the LV and aorta allow for measurement and recording of the transvalvular gradient. Subsequently, a pre-shaped stiff wire (Safari XS, Boston Scientific<sup>TM</sup>) was inserted into the LV through the pigtail catheter. Pre-dilation of the aortic valve was routinely performed in case of self-expandable valve implantation. Transcatheter valve was then delivered over the pre-shaped stiff wire, advanced through the aortic valve using a pigtail, previously placed in the non-coronary cusp as reference. The valve was then deployed and the delivery system retracted. A pigtail was advanced into the left ventricle over the pre-shaped stiff wire to assess the transvalvular gradient. An aortic root angiogram was performed to assess the result. Whenever needed the valve was post-dilated. After the post-dilation, the pigtail was removed from the left ventricle and the Judkin Left 4 guiding catheter was advanced over a J-shaped wire to cannulate the left coronary artery and to perform again the physiological assessment with continuous intracoronary thermodilution.

**Supplementary Table 1. Results from the right heart catheterisation performed in the overall cohort (N=51).**

	<b>Value</b>
<b>HR (bpm)</b>	71 ± 10
<b>RAP (mmHg)</b>	6 ± 6
<b>PCWP (mmHg)</b>	14 ± 7
<b>PAPm (mmHg)</b>	23 ± 8
<b>TPG (mmHg)</b>	9 ± 4
<b>CO (ml/min)</b>	4.8 ± 1.2
<b>AVA (cm<sup>2</sup>)</b>	0.62 ± 0.23
<b>AVAi (cm<sup>2</sup>/m<sup>2</sup>)</b>	0.35 ± 0.11

Data are presented as mean ± SD. Abbreviations: HR: Heart rate; RAP: Right atrial pressure; PCWP: pulmonary capillary wedge pressure; PAPm: mean pulmonary arterial pressure; TPG: total pulmonary gradient; CO: Cardiac output; AVA: Aortic Valve area calculated with Gorling equation; AVAi: AVA indexed.

**Supplementary Table 2. Types and sizes of implanted valves.**

	<b>Number</b>	<b>Size (mm, mean)</b>
<b>Edwards Sapien 3</b>	5 (9.8)	26.7 ± 1.9
- 29 mm	4	
- 26 mm	1	
<b>Abbott Portico</b>	45 (88.2)	26 ± 6
- 23 mm	5	
- 25 mm	9	
- 27 mm	18	
- 29 mm	13	
<b>Medtronic Evolut R</b>	1 (2)	34
- 34 mm	1	

Types of valve implanted in our study. Data are presented as number (%) or mean ± SD.

**Supplementary Table 3. Baseline characteristics of the patients who underwent invasive physiological assessment at follow-up compared to the overall cohort.**

	<b>Cohort at follow-up (N=20)</b>	<b>Overall Cohort (N=51)</b>	<b>p</b>
<b>Gender Male</b>	8 (40.0)	16 (31.4)	0.580
<b>Age</b>	83.5 ± 5	83.7 ± 5	0.625
<b>BMI</b>	26.3 ± 3.8	26 ± 5.3	0.413
<b>Smoking Habitus</b>	3 (15.0)	9 (17.6)	1.000
<b>Hypertension</b>	18 (90.0)	43 (84.3)	0.714
<b>Diabetes</b>	7 (35.0)	16 (31.4)	0.784
<b>Dyslipidemia</b>	17 (85.0)	42 (82.4)	1.000
<b>Afib</b>	1 (5.0)	4 (7.8)	1.000
<b>Afib History</b>	5 (25.0)	17 (33.3)	0.578
<b>Creatinine</b>	1.13 ± 1.12	1.07 ± 0.74	0.413
<b>GFR</b>	66.51 ± 20.39	62.71 ± 19.38	0.347
<b>CKD</b>	4 (20.0)	16 (31.4)	0.394
<b>CAD History</b>	4 (20.0)	10 (19.6)	1.000
<b>Previous PCI</b>	3 (15.0)	8 (15.7)	1.000
<b>Previous MI</b>	0 (0.0)	1 (2.0)	1.000
<b>Pacemaker</b>	0 (0.0)	3 (5.9)	0.554
<b>Angina</b>	0 (0.0)	3 (5.9)	0.554
<b>Dyspnea</b>	19 (95.0)	49 (96.1)	1.000
<b>Syncope</b>	1 (5.0)	6 (11.8)	0.664
<b>Previous HF Hosp.</b>	1 (5.0)	6 (11.8)	0.664
<b>Diuretics</b>	10 (50.0)	27 (52.9)	1.000
<b>Anti Aldosteronics</b>	2 (10.0)	10 (19.6)	0.488
<b>ACEI/ARBS</b>	10 (50.0)	25 (49.0)	1.000
<b>Statins</b>	15 (75.0)	38 (74.5)	1.000
<b>Beta-blockers</b>	8 (40.0)	23 (45.1)	0.793
<b>Calcium Channel Blockers</b>	9 (45.0)	16 (31.4)	0.237
<b>Insulin</b>	0 (0.0)	3 (5.9)	0.554
<b>OAD</b>	7 (35.0)	14 (27.5)	0.571
<b>Anticoagulation</b>	4 (20.0)	14 (27.5)	0.762
<b>Aspirin</b>	7 (35.0)	17 (33.3)	1.000
<b>P2Y<sub>12</sub> inhibitors</b>	4 (20.0)	11 (21.6)	1.000

Data are expressed as mean ± SD or as number (percentage). BMI: body mass index; Afib: Atrial Fibrillation; GFR: glomerular filtration rate; CKD: chronic kidney disease; CAD: coronary artery disease. PCI: percutaneous coronary intervention. MI: myocardial infarction; CCS: Canadian Cardiovascular Society; NYHA: New York Heart Association classification of Heart Failure; HF: Heart Failure; ACEI: angiotensin-converting enzyme inhibitors. ARBs: angiotensin II receptor blockers; OAD: oral antidiabetics;

**Supplementary Table 4. Echocardiographic data at baseline and at follow-up in the overall population.**

	<b>Pre-TAVI (N=51)</b>	<b>Follow-Up (N=51)</b>	<b>P-Value</b>
<b>LVEDD (mm)</b>	45 ± 4	44.67 ± 4.62	0.760
<b>LVEDDI (mm/m<sup>2</sup>)</b>	21 ± 7	21.04 ± 8.86	0.838
<b>IVS (mm)</b>	14 ± 2	12 ± 2	< 0.001
<b>PWT (mm)</b>	10 ± 2	10 ± 2	0.194
<b>RWT</b>	0.48 ± 0.09	0.46 ± 0.08	0.277
<b>LVEDV (ml)</b>	83 ± 20	90 ± 23	0.123
<b>LVEDVi (ml/m<sup>2</sup>)</b>	39 ± 16	41 ± 18	0.428
<b>LVEF (%)</b>	58 ± 5	58 ± 4	0.641
<b>LVM(g)</b>	202 ± 38	175 ± 47	< 0.001
<b>LVMi (g/m<sup>2</sup>)</b>	95 ± 39	82 ± 38	0.107
<b>LVH</b>	37 (72.5)	26 (51.0)	0.041
<b>Peak Aortic Gradient (mmHg)</b>	80 ± 21	16 ± 7	<0.001
<b>Peak aortic velocity (m/s)</b>	4.43 ± 0.40	2.0±0.4	<0.001
<b>AVA (cm<sup>2</sup>)</b>	0.62 ± 0.41	1.04 ± 0.69	<0.001
<b>Mean aortic gradient</b>	51.5 ± 10.2	8.8 ± 4	<0.001

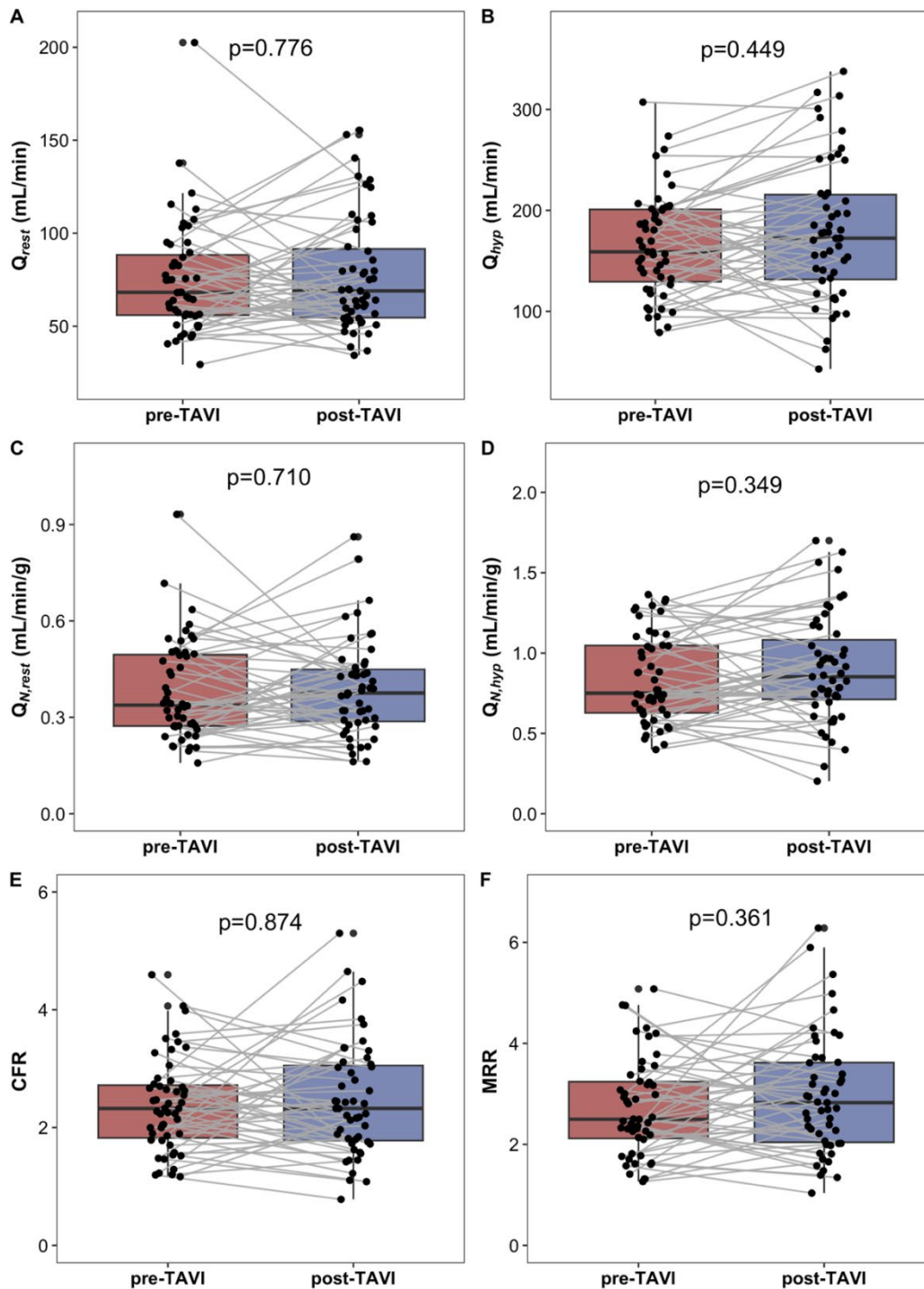
Continuous variables are presented as mean±SD. Categorical variables are presented as number (%). Abbreviations: LVEDD: left ventricular end-diastolic diameter; LVEDDi: left ventricular end-diastolic diameter indexed to BSA; IVS: interventricular septum; PWT: posterior wall thickness; LVEDV: left ventricular end-diastolic volume; LVEDVi: left ventricular end-diastolic volume indexed to BSA; LVEF: Left ventricular ejection fraction; LVM: Left ventricular mass; LVMi: left ventricular mass indexed to BSA; LVH: left ventricular hypertrophy. .

**Supplementary Table 5. Echocardiographic data at discharge.**

	<b>Overall (N=51)</b>
<b>Peak Aortic Gradient (mmHg)</b>	16.55 (4.56)
<b>Mean Aortic Gradient (mmHg)</b>	9.57 (2.66)
<b>Significant AR*</b>	0 (0)
<b>Significant PVL*</b>	1 (2.1)
<b>Significant MR*</b>	1 (2.1)
<b>Significant TR*</b>	2 (4.3)
<b>LVEF (%)</b>	57.32 ± 9.28

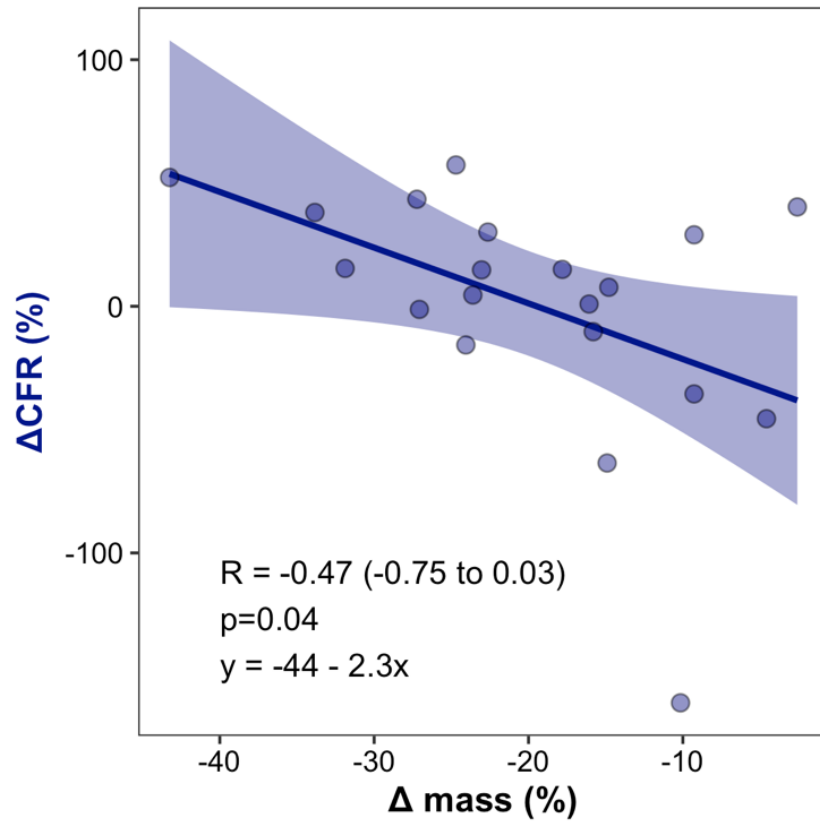
Data are presented as mean ± SD or as number (percentage). AR: aortic regurgitation; PVL: paravalvular leak; MR: mitral regurgitation; TR: tricuspid regurgitation; LVEF: left ventricular ejection fraction.

- ≥ moderate AR/PVL/MR/TR.



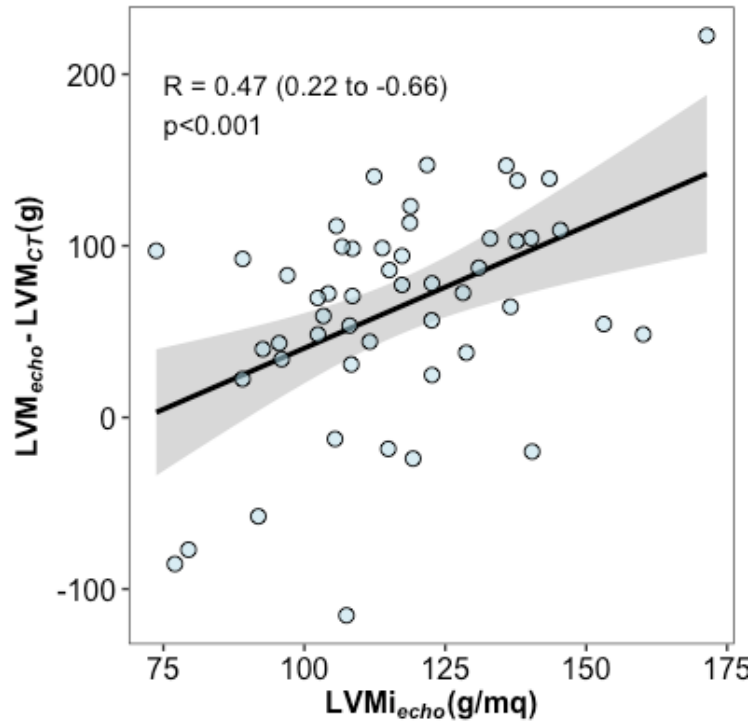
**Supplementary Figure 1.** Absolute flow, myocardial perfusion, CFR and MRR pre- and post-TAVI in the overall population (N=51).

Boxplot with stripchart showing differences between absolute flow and myocardial perfusion at rest ( $Q_{rest}$  and  $Q_{N,rest}$ ) and during hyperaemia ( $Q_{hyp}$ ,  $Q_{N,hyp}$ ) at baseline (pre-TAVI) and at follow-up (panels A to D). In panel E and F are shown the difference pre and post-TAVI of coronary flow reserve (CFR) and microvascular resistance reserve (MRR).



**Supplementary Figure 2.** Correlation between the relative changes in myocardial mass and myocardial perfusion between baseline and follow-up measurements.

Scatter plot with correlation and regression equation between relative changes in CFR and mass before TAVI and at follow up.  $\Delta\text{CFR}(\%)$  represent the relative change in CFR before and after TAVI.  $\Delta\text{mass}(\%)$  represent the relative change in the subtended mass before TAVI and at follow-up expressed as percentage



**Supplementary Figure 3.** Divergence between CT and echocardiography-derived myocardial masses.

Scatter plot with the correlation between the indexed left ventricular myocardial mass derived by echocardiography ( $LVMi_{echo}$ ) and the difference between the left ventricular myocardial mass derived by echocardiography ( $LVM_{echo}$ ) and cardiac computed tomography ( $LVM_{CT}$ ) showing that alongside with the progression of left ventricular hypertrophy (represented by  $LVMi_{echo}$ ) the difference between echocardiography and CT in myocardial mass calculation increases.